19th Australasian Fluid Mechanics Conference
Melbourne, Australia
8-11 December 2014

An Experimental Investigation of the Flow in the Near Wake of a Sharp-edged Strut

C. A. Albarracin and C. J. Doolan.

School of Mechanical Engineering
The University of Adelaide , South Australia 5005, Australia

Abstract

This paper describes an experimental investigation of the coherence function of the turbulent velocity, in the near wake of a two-dimensional sharp-edged strut, at zero angle of attack and at $Re_c = 500,000$, using hot wire anemometry. The paper focuses mainly on the shape of the coherence function as a function of spatial separation. It is found that the spanwise coherence function is well represented by a Gaussian curve, while the wall-normal coherence function is better represented by an exponential curve. For both cases the decay rate is a function of wall-normal distance.

Introduction

Turbulent boundary layer flow over a sharp edged airfoil generates broadband noise, which can be detrimental in a variety of engineering applications, including aircraft, wind turbines and submarines. Understanding the flow over the trailing edge (TE) is paramount for the development of TE noise prediction methodologies, such as the RANS-based Statistical Noise Method (RSNM) [1]. This method requires a model of the turbulent velocity cross-spectrum near the TE. The cross-specrum can be defined in terms of the auto-spectra at each point and the coherence function between the points.

Models for the velocity auto-spectrum in boundary layers are well established [8], but models for cross-spectrum are not. There have been programs to measure two-point statistics in wall bounded flows, including zero pressure gradient (ZPG) turbulent boundary layers [10, 2, 9, 3] and turbulent boundary layers subjected to pressure gradients [5].

However, there have been few attempts to analytically model the turbulent velocity two-point space-time correlation (or its equivalent in the frequency domain, the cross-spectrum) for boundary layers.

Phillips [7] developed a model of the velocity cross correlation based on channel flow DNS data of Kim et al. [6]. The model is a function of spatial separation, a length scale, the Reynolds stresses and mean flow velocity. They conclude that the model should be applicable to turbulent boundary layers as well as for channel flow.

Gavin [3] proposed another model for ZPG turbulent boundary layers based on hot wire measurements. In this work, the correlation volume was modeled as an ellipsoid inclined at an angle θ to the wall. Values were provided for the inclination angle and stretching ratio between the major and minor axes of the ellipsoid, based on best fit to the experimental data. The model requires a convection velocity and the specification of a correlation length.

To the authors' best knowledge, there are no models of the turbulent velocity cross-spectrum for turbulent boundary layers subject to adverse pressure gradients. The main aim of this paper is to measure the streamwise turbulent velocity coherence function in the near wake of an airfoil, and provide the basis to develop a coherence function model, which coupled with the auto-spectrum model of Pope [8] can provide a model for the turbulent velocity cross-spectrum.

Experimental Setup

Experiments were performed in an open-jet low-speed wind tunnel at the University of Adelaide. The tunnel has a rectangular contraction outlet of dimensions 690 mm $\times$ 360 mm. The jet velocity was set at 6.4 m/s and the measured free stream turbulence intensity was $Ti = 0.65\%$. The model used in the experiment (Figure 1) is a 1.2 m chord strut of 25 mm thickness, with a circular leading edge and a wedge-shaped trailing edge with an apex angle of 12 degrees. The trailing edge thickness is 1 mm. The boundary layer was tripped on both sides by a 0.5 mm thick turbulator strip placed at 10% chord.

The model was positioned such that the leading edge coincided with the exit plane of the contraction outlet, and extension plates were fitted to the contraction outlet to ensure the trailing edge of the model was well within the potential core of the jet and measurements were not influenced by the nozzle lip shear layers. A depiction of the experimental setup is shown in Figure 2, with a coordinate system centered at the mid-span of the trailing edge and coinciding with the airfoil chord line. x, y, z are the streamwise, wall-normal and spanwise directions respectively. U is the mean velocity in the streamwise direction and u' is its fluctuating component. A pitot probe was positioned at $\mathbf{x} = (-1200, 84, 0)$ mm to monitor the free stream velocity.

Two TSI 1210-T1.5 single wire probes with wire length of $L = 1.27$ mm and a wire diameter of $d = 3.81\,\mu$m ($L/d \approx 400$) were used, and were operated using an IFA 100 constant temperature anemometer, with an overheat ratio of 1.8. The reference ("fixed") hot wire probe was mounted on a manual traverse with an accuracy of 0.01 mm and was positioned at the center span ($z = 0$) and desired y location before each measurement. The reference probe positions ranged from $y/\delta = 0$ to $y/\delta = 0.8$, where δ is the boundary layer thickness at the TE. The moving hot wire probe was mounted on a TSI 9400 2-axes traverse system, with a positional accuracy of 0.01 mm. The TSI traverse was controlled using the TSI-9400 traverse controller, which was connected to a computer via RS-232 port. When the moving probe was traversed in the wall-normal direction, the reference probe was always the one closer to the wall. All two-point data were taken at 1 mm downstream of the trailing edge ($x = 1$ mm).

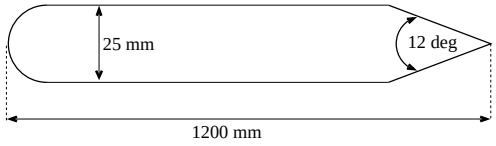

Figure 1: Test case used in the experiments. The model has a circular leading edge and a bevelled trailing edge of 1 mm thickness.

Data were acquired using a NI-PXI4472 data acquisition card, at a sample rate of 20 kHz for 8 seconds. A low-pass filter with a cut-off frequency of 8 kHz was applied to the data prior to digitization to avoid aliasing.

Methodology

The coherence function between two signals x and y is defined as:

$$\gamma^2_{xy}(f) = \frac{|G_{xy}(f)|^2}{G_{xx}(f)G_{yy}(f)} \tag{1}$$

where $G_{xx}(f)$ and $G_{yy}(f)$ are the the auto-spectrum of signals x and y, respectively, and $G_{xy}(f)$ is the cross-spectrum. Rearranging 1, an expression for the cross-spectrum is obtained.

$$|G_{xy}(f)| = \gamma_{xy}(f)\sqrt{G_{xx}(f)G_{yy}(f)} \tag{2}$$

This means that a turbulent velocity cross-spectrum model can be constructed using a model for the auto-spectrum (spectrum at a single point) and a model for the coherence function. When the signal in question is the fluctuating velocity, the auto-spectrum is usually denoted as E. Pope [8] proposed a model for the auto-spectrum given by:

$$E(\kappa) = C_1\varepsilon^{2/3}\kappa_1^{-5/3} f_L(\kappa_1 L) f_\eta(\kappa_1\eta) \tag{3}$$

where C_1 is a constant, κ_1 is the wave number in the x direction and η is the Kolmogorov scale. $L = k^{3/2}/\varepsilon$ is a length scale, where k and ε are the turbulent kinetic energy and dissipation, respectively. The non-dimensional functions f_L and f_η determine the shape of the energy containing range and the dissipation range, respectively. The function f_L is given by:

$$f_L(\kappa_1 L) = \left(\frac{\kappa_1 L}{[(\kappa_1 L)^2 + C_L]^{1/2}}\right)^{5/3+p_0} \tag{4}$$

where p_0 is taken to be 2, and C_L is a positive constant. The function f_η is defined as:

$$f_\eta(\kappa_1\eta) = exp\left(-\beta\left[(\kappa\eta)^4 + C_\eta^4\right]^{(1/4)} - C_\eta\right) \tag{5}$$

The coefficients C_L and C_η are determined by the requirement that $E(\kappa)$ and $2\nu\kappa^2 E(\kappa)$ integrate to k and ε, respectively. To obtain the longitudinal spectrum we can integrate the energy spectrum using:

$$E_{11}(\kappa_1) = \int_{\kappa_1}^{\infty} \frac{E(\kappa)}{\kappa}\left(1 - \frac{\kappa_1^2}{\kappa^2}\right) d\kappa \tag{6}$$

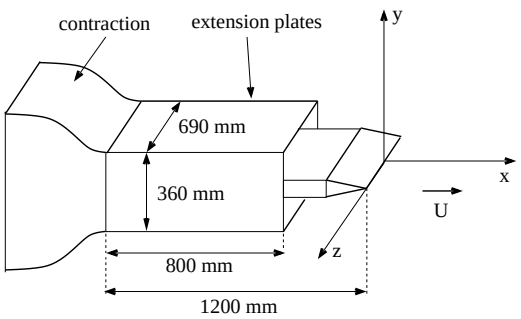

Figure 2: Schematic of the wind tunnel contraction with extension plates and model used in the experiments. The coordinate system was centered at the trailing edge of the model at the mid span point.

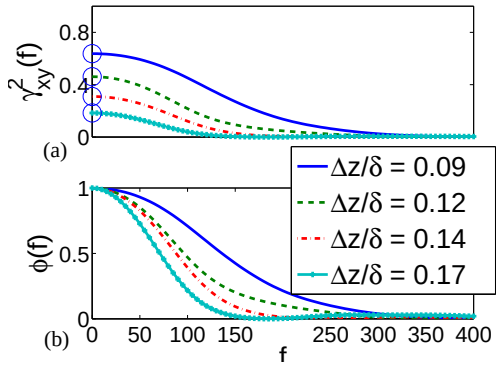

Figure 3: Decomposition of Coherence function into frequency and spatial components. $y/\delta = 0.39$.

The auto-spectrum model of Pope [8] has been shown to produce a good fit to a wide range of turbulent flow data, including grid turbulence, channel flow and turbulent boundary layers. To transform this auto-spectrum model into a cross-spectrum model, a model for the coherence function is required.

The coherence function γ^2_{xy} is a function of both frequency and spatial separation. Two possible approaches can be taken to investigate the behavior of the coherence function; namely, keeping the frequency constant and observing its dependency on spatial separation, or keeping the spatial separation constant and observing its variation with frequency. This paper focuses on the former.

It is assumed that the coherence function can be separated into a spatial component and a frequency component as:

$$\gamma^2_{xy}(f, \Delta\mathbf{x}) = \psi(\Delta\mathbf{x})\phi(f) \tag{7}$$

Where $\phi(f)$ is a normalized frequency dependent component with $\phi(f=0) = 1$, and $\psi(\Delta\mathbf{x})$ has the amplitude of the DC component of γ^2_{xy}. This can be better understood by inspecting Figure 3. Figure 3(a) shows $\gamma^2_{xy}(f, \Delta z/\delta)$ for $\Delta z/\delta = (0.09, 0.12, 0.14, 0.17)$ at $y/\delta = 0.39$ and $x = 1$mm for our test case. The circles mark the DC component $\psi(\Delta z)$ of the coherence function at each probe separation. The normalized frequency component $\phi(f)$ is shown in Figure 3(b). By multiplying $\psi(\Delta z)$ and $\phi(f)$, $\gamma^2_{xy}(f, \Delta z/\delta)$ is recovered.

Furthermore, it is assumed that $\psi(\Delta\mathbf{x})$ can be separated into orthogonal components as:

$$\psi(\Delta\mathbf{x}) = \psi_x(\Delta x)\psi_y(\Delta y)\psi_z(\Delta z) \tag{8}$$

The effects of spatial separation in the wall-normal direction and in the spanwise direction are studied separately. The behavior of the coherence function with streamwise spatial separation could not be investigated due to probe interference effects.

Results

The mean and RMS velocity profiles were measured at various locations both upstream and downstream of the trailing edge in order to investigate the evolution of the boundary layer and wake. Figure 4 shows the mean velocity profiles at different locations in the wake, as a function of y/δ, were δ is the boundary layer thickness at the trailing edge. The figure shows the outer half of the boundary layer remains unchanged up to $x/c = 0.067$, where $c = 1200$ mm is the airfoil chord, but

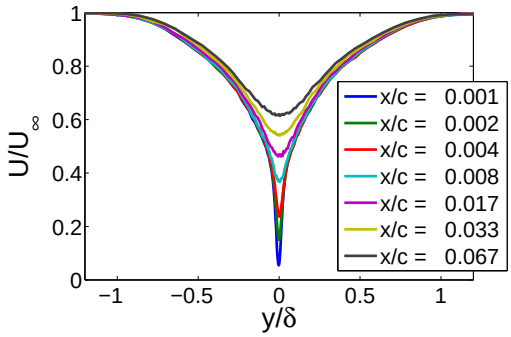

Figure 4: Mean velocity profiles taken at various distances x/c from the trailing edge.

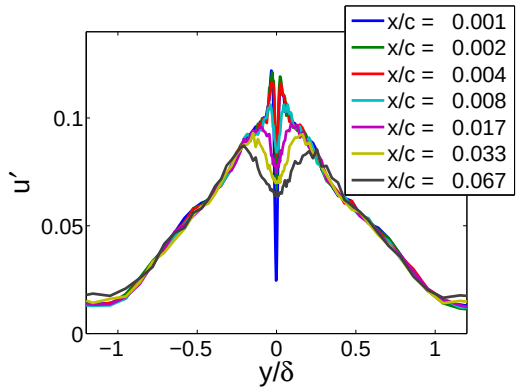

Figure 5: RMS velocity profiles taken at various distances x/c from the trailing edge.

the velocity deficit is quickly recovered along the centerline of the wake. This is consistent with the observations of [4] for a NACA 0012 airfoil at zero angle of attack.

Similarly, the RMS velocity profiles remain unchanged in the outer layer, as shown in figure 5. The dip in turbulence intensity in the center line of the wake and the peaks on either side become smaller and less sharp as x/c increases. This is expected, as the wall is no longer present to create more turbulence through viscous effects and both boundary layers gradually merge across the centerline of the wake.

Figure 6 shows the auto-spectral density plotted with Kolmogorov scaling for a range of values y/δ, together with Pope's model spectrum for $y/\delta = 0.13$. When plotted this way, the data shows a very good colapse for $\kappa_1\eta \geq 10^{-1}$. It is also clear that Pope's model provides a credible representation of the data. The data are well resolved down to the Kolmogorov scale η.

Figure 7 shows the spatial component of the coherence function as a function of wall-normal separation, $\psi_y(\Delta y)$, and an empirical exponential curve defined by a least squares approach. The wall-normal distance of the reference probe is $y_1/\delta = 0.39$. The same procedure was employed for a range of fixed probe positions y_1/δ , and the decay rate was obtained for each position. An empirical curve was found for the decay rate at each wall-normal position, as shown in Figure 8. The data are well represented by:

$$\psi_y(\Delta y) = \exp(-b_y(\Delta y/\delta)) \tag{9}$$

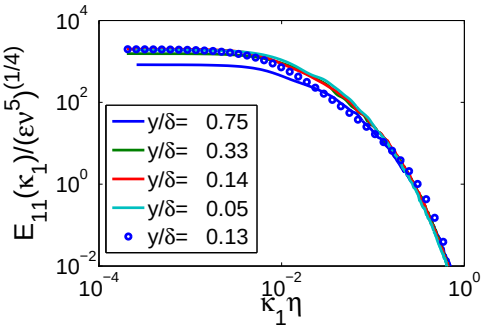

Figure 6: Normalised auto-spectral density of streamwise fluctuating velocity at various wall-normal distances taken at 1 mm downstream from the trailing edge. Solid lines are experimental data, symbols are Pope's model spectrum.

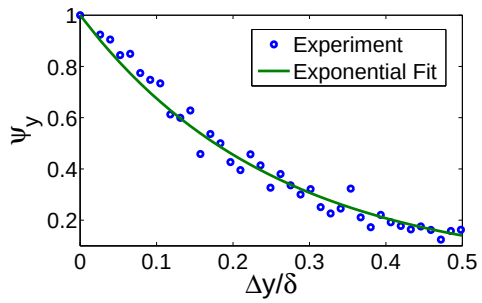

Figure 7: Spatial component of the coherence function with probe separation in the wall-normal direction. Reference probe location $y_1/\delta = 0.39$. Data taken at 1mm downstream of the trailing edge.

where the decay rate b_y is given by:

$$b_y = \frac{a_y}{(y/\delta)^{p_y}} \tag{10}$$

with the empirical constants $a_y = 2.7655$ and $p_y = 0.3049$ being determined using a least squares approach.

Similar to the wall-normal case, $\psi_z(\Delta z)$ was measured at various distances from the wall, ranging from $y/\delta = 0$ to $y/\delta = 0.8$, and a curve fitting procedure was employed to determine its functional dependency on spatial separation. The data are well represented by a Gaussian function, given by:

$$\psi_z(\Delta z) = \exp(-b_z(\Delta z/\delta)^2) \tag{11}$$

where the decay rate is given by:

$$b_z = \frac{a_z}{(y/\delta)^{p_z}} \tag{12}$$

with the empirical constants $a_z = 24.43$ and $p_z = 0.6541$. Figure 9 shows $\psi_z(\Delta z)$ with a Gaussian curve fit for $y/\delta = 0.39$. The decay rate as a function of distance to the wall is shown in Figure 10 together with equation 12, which is shown to provide a good fit to the data.

Conclusion and Future Work

The streamwise velocity coherence function was measured in the near wake of a flat strut with a bevelled trailing edge. The boundary layer was fully turbulent and subject to an adverse

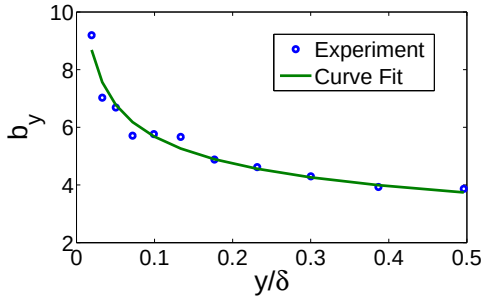

Figure 8: Decay rate of the spatial component of the coherence function with probe separation in the wall-normal direction. Reference probe location $y_1/\delta = 0.39$. Data taken at 1mm downstream of the trailing edge. Symbols: experimental data. Line: equation 10.

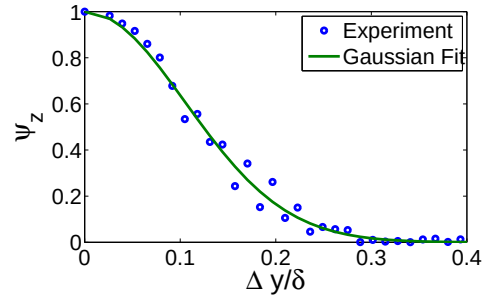

Figure 9: Spatial component of the coherence function with probe separation in the spanwise direction. Data taken at $y/\delta = 0.39$ and 1mm downstream of the trailing edge.

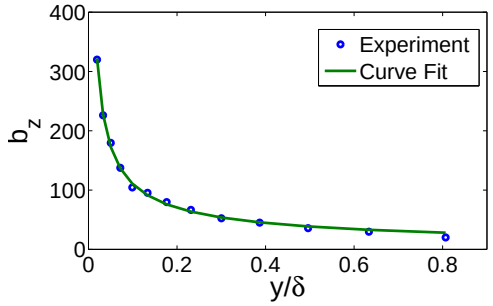

Figure 10: Decay rate of the spatial component of the coherence function with probe separation in the spanwise direction. Symbols: Data taken at $y/\delta = 0.39$ and 1mm downstream of the trailing edge. Line: equation 12

pressure gradient in the aft section of the strut. Measurements in the near wake of mean and RMS velocity profiles, auto-spectral density and coherence function of u' are presented. It is found that the for $y/\delta \geq 0.5$ the boundary layer is not significantly affected by the absence of the wall up to $x/c = 1.067$. The model of Pope provides a credible fit to the auto-spectral density of u'. It was found that the spatial component of the coherence function in the wall-normal direction can be modeled by an exponential function. In the spanwise direction, the spatial component of the coherence function can be modeled as a Gaussian function. The decay rates of these functions depend on the distance to the wall. Empirical expressions are provided for the decay rates in both spanwise and wall-normal directions.

For a coherence function model to be complete, the frequency dependency of the coherence function needs to be included. This is the subject of ongoing research. Future work is intended to combine a complete model for the coherence function with Pope's auto-spectrum model in order to develop a cross-spectrum model of u' that can be used in trailing edge noise calculations.

References

[1] Albarracin, C., Doolan, C., Jones, R., Hansen, C., Brooks, L. and Teubner, M., A RANS-based statistical noise model for trailing edge noise, in *Proceeding of the 18th AIAA/CEAS Aeroacoustics Conference, AIAA Paper*, 2012, volume 2181.

[2] Favre, A. J., Gaviglio, J. J. and Dumas, R., Space–time double correlations and spectra in a turbulent boundary layer, *Journal of Fluid Mechanics*, **2**, 1957, 313–342.

[3] Gavin, J., *Unsteady forces and sound caused by boundary layer turbulence entering a turbomachinery rotor*, Ph.D. thesis, The Pennsylvania State University, University Park, PA., 2002.

[4] Ghaemi, S. and Scarano, F., Counter-hairpin vortices in the turbulent wake of a sharp trailing edge, *Journal of Fluid Mechanics*, **689**, 2011, 317–356.

[5] Harun, Z., *The structure of adverse and favourable pressure gradient turbulent boundary layers*, Ph.D. thesis, Department of Mechanical Engineering, University of Melbourne, 2012.

[6] Kim, J., Moin, P. and Moser, R., Turbulence statistics in fully developed channel flow at low Reynolds number, *Journal of Fluid Mechanics*, **177**, 1987, 133–166.

[7] Phillips, W. R. C., Eulerian spacetime correlations in turbulent shear flows, *Physics of Fluids*, **12**, 2000, 98–108.

[8] Pope, S. B., *Turbulent flows*, Cambridge university press, 2000.

[9] Tritton, D. J., Some new correlation measurements in a turbulent boundary layer, *Journal of Fluid Mechanics*, **28**, 1967, 439–462.

[10] Tutkun, M., Georgeb, W., Delvillec, J., Stanislasd, M., Johanssone, B., Foucautd, J. and Coudertd, S., Two-point correlations in high Reynolds number flat plate turbulent boundary layers, *Journal of Turbulence*, **10**, 2009, 1–23.